Graphene-Hexagonal Boron Nitride Work Function Response to Uniform Planar Deformations: An ab initio DFT Study

A Thesis Presented to the Department of Theoretical and Applied Physics

African University of Science and Technology

In Partial Fulfillment of the Requirements for the Degree of Master of Science

By

Jesutofunmi Ayo FAJEMISIN

40769

African University of Science and Technology

P.M.B 681, Garki, Abuja F.C.T

Nigeria.

April, 2021

Certification

This is to certify that this study was carried out by Jesutofunmi Ayo FAJEMISIN, with student identification number 40769 under the supervision of Dr Abdulhakeem Bello and Dr Okikiola Olaniyan.

Graphene-Hexagonal Boron Nitride Work Function Response to Uniform Planar Deformations: An ab initio DFT Study

By

Jesutofunmi Ayo Fajemisin

A Thesis Presented to the Department of Theoretical and Applied Physics

RECOMMENDED: _____

Supervisor: Dr. Abdulhakeem Bello

_____

HOD: Prof Kenfack Anatole

APPROVED: _____

Chief Academic Officer

ABSTRACT

A two-dimensional hybrid material with graphene and hexagonal boron (h-BN) domain is considered as viable material for future generations of flexible electronic devices due to the tunable band gap, excellent mechanical and thermal properties. There is a growing interest that this hybrid material could be used for low contact barrier electrodes and various field emitting devices yet no report till date as presented the work function of the material. Tuning the work function is a known approach to reduce the contact barriers and obtain electrodes with low contact resistance. In this work, we calculated, using density functional theory, the stability, band gap, and work function of a 2D hybrid material in which graphene (h-BN) is embedded h BN (graphene). We achieved band gap tuning by varying the graphene (h-BN) domain in h-BN (graphene), while the work function was engineered by applying uniform strains to the most stable form of the hybrid material. The cohesive energy results show that the hybrids are stable with respect to pristine h-BN.

ACKNOWLEDGEMENT

I would like to express my heartfelt gratitude to the Almighty God for His protection and guidance during this project. I'd like to express my heartfelt appreciation to Dr. Abdulhakeem Bello and Dr Okikiola Olaniyan for their inspiring leadership and never-ending support in helping me finish this project. A special thanks to the Head of Department, Prof. Anatole Kenfack for his guidance during this program. To my mentors, Dr. Omololu Akin-Ojo and Dr. Ketevi Assamagan, I can't take your love and support for granted. I also appreciate all the faculty members who taught me at the African University of Science and Technology (AUST) for the knowledge they imparted in me without hesitation. Finally, my sincere gratitude to my family (mum and siblings) and friends – Bonaventure, Kabir, Gyang, Denis, Samuel, Oluwanisola and George. Thank you for the encouragement at those low moments. You are loved.

DEDICATION

This project is dedicated to my late father, Adekunle Fajemisin.

Table of Contents

CHAPTER ONE

INTRODUCTION

1.1 Graphene

In 2004, two researchers at the University of Manchester, Andre Geim and Kostya Novoselov successfully isolated graphene from graphite for the first time [1]. This experiment won the Nobel Prize in Physics in 2010. Graphene has amazing properties that has made it a promising material for diverse applications in electronics, energy storage, biomedical, composite and coating etc. [2]. Graphene is a one-atom thick layer of carbon atoms with sp^2 hybrid orbital tightly bound in a two-dimensional hexagonal honeycomb lattice. Graphite is formed by stacking many layers of graphene on top of one another. The strong C=C bonding makes graphene to have a stable structure and excellent mechanical properties with bond length equals to 1.42 Å. It is the thinnest and the strongest material ever known. It has high electron mobility, zero effective mass and can travel for microstates without scattering at room temperature. Its electrical conductivity is 13 times better than copper, excellent optical properties – absorbs only 2.3% of reflecting light. It is both stiff and elastic and can stretch to about 25% of its original length. It has a high thermal conductivity than any other material. As mentioned earlier, graphene has a hexagonal crystal lattice. Its lattice vectors are:

$$\overrightarrow{a_1} = \frac{a}{2}(3, \sqrt{3}) ; \qquad \overrightarrow{a_2} = \frac{a}{2}(3, -\sqrt{3}) \qquad (1)$$

Reciprocal lattice vectors

$$\overrightarrow{b_1} = \frac{2\pi}{3a}(3, \sqrt{3}) ; \qquad \overrightarrow{b_2} = \frac{2\pi}{3a}(3, -\sqrt{3}) \qquad (2)$$

Figure 1.2 represents the Brillouin zone with special high symmetry points K, K' and M with the wave vectors[3]:

$$\overrightarrow{K'} = \left(\frac{2\pi}{3a}, \frac{2\pi}{3\sqrt{3}a}\right) \quad \vec{K} = \left(\frac{2\pi}{3a}, -\frac{2\pi}{3\sqrt{3}a}\right) \quad M = \overrightarrow{K'} = \left(\frac{2\pi}{3a}, 0\right) \qquad (3)$$

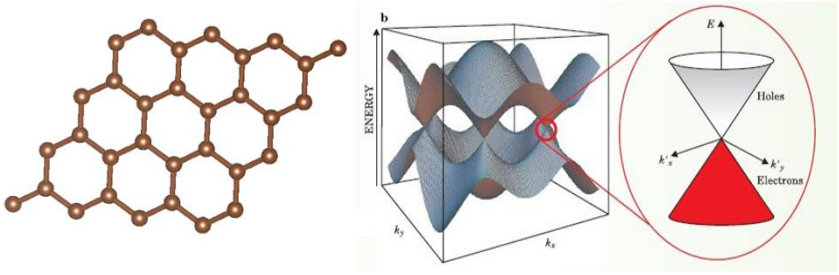

Figure 1.1: (a) crystal structure of graphene (b) Electronic structure of graphene

Graphene is a zero-band gap semiconductor. At the K-point, where the valence π-band and conduction π*-band with a linear wave number dependency meet each other, the zero-band distance property of graphene's band structure emerges. The Dirac point is another name for this point. The function of massless electrons at the Fermi level is shown by the linear dispersion of the π-band and the π*-band at the Fermi level. The Fermi energy of these massless electrons is about 1/300 of the speed of light [4].

1.2 Hexagonal Boron Nitride

Hexagonal boron nitride (h-BN), sphalerite boron nitride (β-BN), and wurtzite boron nitride are the three main allotropes of boron nitride (δ-BN). Hexagonal Boron Nitride has a layered structure, with boron and nitrogen atoms bound by tight covalent bonds in plane and kept together by van der Waals forces within each layer. As compared to strongly conductive

graphene, h-BN has a graphene-like structure with a 5.0 eV band difference. It's also thermally conductive, which makes it appealing for a variety of electronic applications and insulating filter material for polymer. With a bond length of 1.45, the B-N bond is covalent. The hexagonal crystal structure has a high thermal and chemical stability. It can withstand temperatures of over 1000 °C in air, 1400 °C in vacuum, and up to 2850 °C in an inert environment without decomposing. It's also a good dielectric material for electronic devices that generate heat [5], [6].

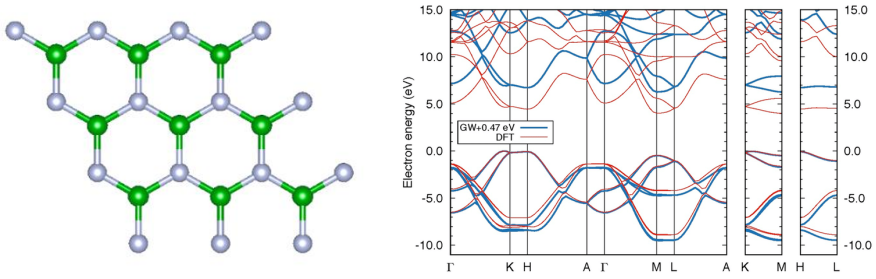

(a) (b)

Figure 1.2 – (a) Crystal structure of h-BN (b) Band Structure of h-BN

1.3 Methods of tuning the properties of graphene

There are existing techniques for tuning the properties of graphene:

- Hydrogenation
- Molecular Adsorption
- Chemical Substitution
- Graphene-Substrate Hybrid Structures

Hydrogenation[7] involves the addition of hydrogen atom pairs to compounds. It is the simplest possible chemical modification of graphene.

Molecular adsorption [8] is accomplished by a significant exchange of electrons between the surfaces of the adsorbent and the adsorbate to form a covalent or ionic bond.

As a result, chemical adsorption may not be fully reversible, and regeneration may take a lot of energy.

Chemical Substitution [9] – The complex electronic and spin structures of graphene can be efficiently tuned by substituting foreign elements like boron, sulfur, and fluorine, and substituted or decorated graphene as promising materials have been successfully used in electrical, optical, and catalytic fields.

Graphene-Substrate Hybrid Structures [10] **–** This involves different configurations of graphene-substrate hybrid structures. It is known that there is a weak interaction between the graphene and the substrate. The band gap of graphene is strongly affected but the intrinsic mechanical and physical properties of graphene do not change remarkably.

1.4 Aims and Objectives

1.4.1 Aims

- To create a stable 2D Nano semiconductor with a tuneable work function for nano electronic devices.
- To develop a model that gives the relationship between work function and applied strain on 2D nano semiconductors
- Transform graphene and h-BN to semiconductors

1.4.2 Objectives

- Design a 2D graphene and h-BN nano composite material
- Investigate the effect of concentration of h-BN and graphene in the hybrid on the electronic properties.
- Apply a first principle in the framework of DFT method to calculate the stability, structural and electronic properties of the hybrid systems.

CHAPTER TWO

LITERATURE REVIEW

2.1 Graphene

Different articles have reported diverse ways and measures to engineer the electronic properties of graphene say band gap, work function, cohesive energy, etc.

Mohammed H. Mohammed, 2017 [11] studied the electronic properties of graphene nanosheet with and without various concentrations of phosphorus in various sites by using the first principles of the density functional theory method. A supercell of 72 atoms was studied using GGA exchange correlation. The Brillion zone was sampled using 2x2x1 Monkhorst-Pack grid with 80 Ry cut-off energy. The results showed that doping one phosphorus atom in the graphene sheet alter the band gap from 0 to 0.0067 eV, 0 to 0.00728 and 0 to 0.00874 eV depending on the location of the dopant. Therefore, the electronic band gap of GNS depends on the concentration of the impurities and the location of the impurities. Also, Total energy is affected and reduced with these impurities.

Furthermore, Yingke Zhou et. al., 2015 [12] used DFT calculations to investigate the N-doping effect on the electric properties(capacitance) of graphene. The band structure and density of states of the graphitic and non-graphitic N-doped graphene models were reported. The Dirac point shift, band gap opening, DOS increasing creates modification in the electronic structure which results in changes in the capacitance. It was reported that when the heteroatoms are graphitic, the p_z electron of the substituted heteroatoms anticipates the large π-conjugate bond system of graphene and the p_x and p_y electrons sp^2-hybridize with the s-orbital and form σ -bonds with the adjacent three carbon atoms, and, resulting in increased electrical double layer capacitance (C_{dl}). For non-graphitic doping, a sharp peak contributed by p_x and p_y electrons appears at about ≈0.7 V below the Fermi level corresponding to the localized excess electron, which can be easily involved in the

proton and electron transfer processes, resulting in increased Faradaic pseudocapacitance of graphene.

2.2 Hexagonal Boron Nitride

Razieh Beiranvand and Shahoo Valedbagi, 2003 [13] focused on the electronic and linear properties of the hexagonal BN nanosheet. The average B-N bond length is 1.43 Å and the total density of state and corresponding electronic band structure were reported. The results shows that it has semiconducting properties with a wide band gap of 4.95 eV. It was also reported that there are two main peaks for the imaginary part of dielectric tensor in both E∥x and E∥z directions. They also presented that optical conductivity in electric field parallel and perpendicular to the h-BN nanosheets starts with a small gap of 2.92 and 6.73 (eV) respectively, which confirms that this nanosheets as semiconductors and also has an isotropic characteristic along these two polarizations.

Similarly, Bing Huang and Hoonkyung Lee, 2012 [14] studied the structural and electronic properties of vacancy defects and carbon impurity in hexagonal boron nitride (h-BN) by using both normal GGA calculations and advanced hybrid functional calculations. It was observed that the highest negative charge states of defects are largely determined by the nearly free electron states at the conduction band minimum. Also, the Nearly Free Electrons (NFE) at the conduction band minimum becomes even lower in energy when the results obtained using PBE calculations were compared to the HSE calculations. For single boron vacancy, the energy difference between the defect levels and VBM are 0.5, 0.5, and 1.2 eV for levels 1, 2, and 3, respectively (PBE) while it is 2.5, 2.1, and 3.2eV (HSE). The formation energies of V.B under PBE and HSE calculations are 7.38 and 7.65 eV, respectively, indicating that PBE is good enough for calculating the

formation energy of neutral V.B. For single Nitrogen vacancy, the formation energy of V.N is 7.70 eV which is 0.77 eV lower than that gotten from HSE calculation.

2.3 Graphene-Hexagonal Boron Nitride Hybrid System

First principle calculation was used by Man Zhao et. al., 2014 [15] to study the electronic and magnetic properties of the hybrid structures of BN and graphene. It was observed that the electronic and magnetic states of the hybrid structures are extremely sensitive to hydrogen adsorption. The mid-gap states cross Fermi levels can be produced or suppressed upon hydrogen adsorption, dependent on whether the numbers of Boron (B) and Nitrogen (N) atoms replaced by Carbon (C) atoms are the same or not. It was reported that the adsorption of a hydrogen atom inject an electron to the hybrid system. If the difference between the number of the extra-nuclear electrons of the hybrid system and that of pure BN sheet is reduced because of the injected electrons, the mid-gap states will be suppressed, and vice versa. However, the mid-gap states are insensitive to the adsorption sites since the injected electrons can move freely rather than been localized at a certain atom. The adsorbed hydrogen atom induces a transition in the material from the semiconducting state to the metallic state, which provides a potential method to engineer the band gap of this two-dimensional hybrid structure. The spin-resolved band gap and electronic density of states are also analyzed. The results illustrated that the magnetism of the hybrid structures changes with the adsorbed H atom. As for the hybrid structure with different numbers of B and N atoms replaced by C atoms, the hybrid structures are magnetic but will disappear or be reduced due to the H adsorption. As for the hybrid structures with the same numbers of B and N atoms replaced by C atoms, they will be transformed from non-magnetic to magnetic upon H adsorption but is insensitive to the adsorption sites.

Also, Olaniyan et.al., 2020 [16] studied the first principle calculations of the hybrid structure consisting of in-plane graphene and hexagonal boron nitride (h-BN). It was reported that the influence of graphene or h-BN domain size on the atomic geometries, electronic properties, and thermodynamic properties of graphene/h-BN hybrid structures with a zigzag interface. Also, the graphene domain size reduces the band gap, which is tunable up to 1.01 eV. The Debye temperature reacts differently: it rises as the graphene domain grows in size. The graphene and h-BN values limit the thermodynamic properties of the hybrid system, which can be tuned to converge to either graphene or h-BN based on the scale of the graphene domain.

2.4 Work function of Graphene

Hollow sites, Bridge sites, and Top sites – was used to investigate the structural properties of p-doped graphene by placing p-dopant atoms at the three adsorption sites. Merid Legesse et. al., 2020 [17]–The B-site has been shown to be the most stable adsorption site for non-metal elements in groups V and VI, whereas Group VII elements tend to be adsorbed at the graphene top (T) sites. The effect of non-metal adatoms (p-dopants) adsorption on the work function was investigated at various dopant concentrations. The work function of graphene was thus stated to increase from 4.38 eV for pristine content to 5.76 eV and 5.71 eV for Chlorine (Cl)–doped and Boron (Br)–doped graphene, respectively (at a dopant concentration of 4%). Charge transfer from graphene to non-metal adatoms induces electron depletion at the graphene plane, lowering the Fermi level and increasing the work function of the device, according to the authors. The stability conditions for absorbed halogen adatoms on graphite was also investigated.

CHAPTER THREE

METHODOLOGY

3.1 Time Independent Schrodinger Equation

The interactions of electrons and nuclei determine the properties of materials. Quantum mechanics is needed to describe such interactions. To explain the properties of a well-defined set of atoms. One of the most important things we want to know about these atoms is their energy and, more importantly, how the motion of the electrons and ions in the system affects its energy. The Time Independent Schrodinger equation (TISE) perfectly describes the dynamics of ions and electrons in an atom.

$$\widehat{\boldsymbol{H}}\boldsymbol{\psi_i} = \boldsymbol{E_i}\boldsymbol{\psi_i} \qquad \textbf{(3.1)}$$

Where $\widehat{\boldsymbol{H}} = \widehat{\boldsymbol{T}} + \widehat{\boldsymbol{V}}$ is called the Hamiltonian of the system which is given as the sum of the kinetic energy and the potential energy of the system.

We considered atoms consisting of valence and core electrons. Since the valence electrons are responsible for bonding and the properties of the system, we therefore combine the core electrons and nucleus and term them ions. The Hamiltonian comprises of the kinetic energy of the ions and electrons and the potential energy of the ion-ion, electron-electron and electron-ion interactions.

For a many body system, the Hamiltonian is given as:

$$\widehat{\boldsymbol{H}} = -\frac{\hbar^2}{2\boldsymbol{m_e}}\sum_{\boldsymbol{i}=1}^{\boldsymbol{N}}\boldsymbol{\nabla_i^2} - \hbar^2\sum_{\boldsymbol{I}=1}^{\boldsymbol{M}}\frac{\boldsymbol{\nabla_I^2}}{2\boldsymbol{M_I}} + \frac{1}{2}\sum_{\boldsymbol{i}\neq\boldsymbol{j}}^{\boldsymbol{N}}\frac{\boldsymbol{e^2}}{|\vec{\boldsymbol{r}}_{\boldsymbol{i}}-\vec{\boldsymbol{r}}_{\boldsymbol{j}}|} - \sum_{\boldsymbol{i}=1}^{\boldsymbol{N}}\sum_{\boldsymbol{I}=1}^{\boldsymbol{M}}\frac{\boldsymbol{Z_i e^2}}{|\vec{\boldsymbol{r}}_{\boldsymbol{i}}-\vec{\boldsymbol{R}}_{\boldsymbol{I}}|} + \frac{1}{2}\sum_{\boldsymbol{I}\neq\boldsymbol{J}}^{\boldsymbol{M}}\frac{\boldsymbol{Z_I Z_J e^2}}{|\vec{\boldsymbol{R}}_{\boldsymbol{I}}-\vec{\boldsymbol{R}}_{\boldsymbol{J}}|} \qquad \textbf{(3.2)}$$

$$\widehat{\boldsymbol{H}} = \widehat{\boldsymbol{T}}_{\boldsymbol{elec}} + \widehat{\boldsymbol{T}}_{\boldsymbol{ion}} + \widehat{\boldsymbol{V}}_{\boldsymbol{ion-elec}} + \widehat{\boldsymbol{V}}_{\boldsymbol{elec-elec}} + \widehat{\boldsymbol{V}}_{\boldsymbol{ion-ion}} \qquad \textbf{(3.3)}$$

The wavefunction of the many body system is given as:

$$\boldsymbol{\psi_i = \psi_i(\vec{r}_1, \ldots . \vec{r}_N,\ \sigma_1, \ldots ,\ \sigma_N : \vec{R}_1, \ldots , \vec{R}_M,\ \delta_1 \ldots , \delta_M)} \qquad \textbf{(3.4)}$$

Solving the TISE for a many-body system is very difficult due to the many degrees of freedom of the wavefunction and the multiplicity of this wavefunction in the electron-electron interaction is very hard to compute.

3.2 The Rayleigh-Ritz Variational Principle

Given the Hamiltonian of a system, the expectation value of the Hamiltonian is always greater than or equal to the ground state energy of the system.

$$\mathbf{Q(\psi) = \frac{\langle \psi | H | \psi \rangle}{\langle \psi | \psi \rangle} \geq E_o} \qquad \textbf{(3.5)}$$

Suppose $|\psi\rangle$ is expressed in terms of a variable parameter η , then Q can be made to get close E_o by:

$$\boldsymbol{\frac{\partial Q}{\partial \eta} = 0} \qquad \textbf{(3.6)}$$

Using the method of Lagrange multiplier

$$\boldsymbol{\delta[\langle \psi | H | \psi \rangle - \lambda \mathrm{g}] = 0} \qquad \textbf{(3.7)}$$

where **g** is the constraint

3.3 Adiabatic or Born-Oppenheimer Approximation

This approximation is based on the assumption that the electronic motion and the nuclear motion in molecules can be treated separately. Ions are much heavier than electrons, hence, the kinetic energy of the ions is negligible and the ion-ion interaction term is held constant.

$$\widehat{\boldsymbol{H}} = -\frac{\hbar^2}{2\boldsymbol{m_e}}\sum_{\boldsymbol{i=1}}^{\boldsymbol{N}} \boldsymbol{\nabla_i^2} - \hbar^2 \sum_{\boldsymbol{I=1}}^{\boldsymbol{M}} \frac{\boldsymbol{\nabla_I^2}}{2\boldsymbol{M_I}} + \frac{\mathbf{1}}{\mathbf{2}} \sum_{\boldsymbol{i\neq j}}^{\boldsymbol{N}} \frac{\boldsymbol{e^2}}{|\vec{\boldsymbol{r}}_{\boldsymbol{i}} - \vec{\boldsymbol{r}}_{\boldsymbol{j}}|} - \sum_{\boldsymbol{i=1}}^{\boldsymbol{N}} \sum_{\boldsymbol{I=1}}^{\boldsymbol{M}} \frac{\boldsymbol{Z_i e^2}}{|\vec{\boldsymbol{r}}_{\boldsymbol{i}} - \vec{\boldsymbol{R}}_{\boldsymbol{I}}|} + \frac{\mathbf{1}}{\mathbf{2}} \sum_{\boldsymbol{I\neq J}}^{\boldsymbol{M}} \frac{\boldsymbol{Z_I Z_J e^2}}{|\vec{\boldsymbol{R}}_{\boldsymbol{I}} - \vec{\boldsymbol{R}}_{\boldsymbol{J}}|} \qquad \textbf{(3.8)}$$

The above Hamiltonian becomes

$$\widehat{\boldsymbol{H}}_{\boldsymbol{elec}} = \widehat{\boldsymbol{T}}_{\boldsymbol{elec}} + \widehat{\boldsymbol{V}}_{\boldsymbol{ion-elec}} + \widehat{\boldsymbol{V}}_{\boldsymbol{elec-elec}} \qquad \textbf{(3.9)}$$

$$\widehat{\boldsymbol{H}}_{\boldsymbol{elec}} = -\frac{\hbar^2}{2\boldsymbol{m_e}}\sum_{\boldsymbol{i=1}}^{\boldsymbol{N}} \boldsymbol{\nabla_i^2} - \sum_{\boldsymbol{i=1}}^{\boldsymbol{N}} \sum_{\boldsymbol{I=1}}^{\boldsymbol{M}} \frac{\boldsymbol{Z_i e^2}}{|\vec{\boldsymbol{r}}_{\boldsymbol{i}} - \vec{\boldsymbol{R}}_{\boldsymbol{I}}|} + \frac{\mathbf{1}}{\mathbf{2}} \sum_{\boldsymbol{i\neq j}}^{\boldsymbol{N}} \frac{\boldsymbol{e^2}}{|\vec{\boldsymbol{r}}_{\boldsymbol{i}} - \vec{\boldsymbol{r}}_{\boldsymbol{j}}|} \qquad \textbf{(3.10)}$$

It can be seen that the Hamiltonian is now a function of the position of the electrons only. Therefore, our TISE can be written as

$$\widehat{\boldsymbol{H}}_{\boldsymbol{elec}}\boldsymbol{\psi}_{\boldsymbol{elec}}(\vec{\boldsymbol{r}}_{\mathbf{1}}, \vec{\boldsymbol{r}}_{\mathbf{2}}, \dots) = \boldsymbol{E}_{\boldsymbol{elec}}\boldsymbol{\psi}_{\boldsymbol{elec}}(\vec{\boldsymbol{r}}_{\mathbf{1}}, \vec{\boldsymbol{r}}_{\mathbf{2}}, \dots) \qquad \textbf{(3.11)}$$

With Bon-Oppenheimer approximations, the wavefunction still has many degrees of freedom which is computationally expensive to solve. Other approximations are formulated to solve the above equation.

3.4 Hatree Approximation

Here, we write the trial many-body wavefunction

$$\boldsymbol{\psi(x_1 \cdots x_n) = u_1(x_1)u_2(x_2)\cdots u_n(x_n)} \quad \textbf{(3.12)}$$

Where each electron is treated as independent and they interact only via the mean-field Coulomb potential.

The Hamiltonian is written as

$$\boldsymbol{\hat{H}_{elec}(x_1 \cdots x_n) = \sum_{i=i}^{N} H(i) + \frac{1}{2}\sum_{i,j}' V(i,j)} \quad \textbf{(3.13)}$$

Applying constraint

$$\boldsymbol{\int \psi^*(x_1, \cdots x_n)\psi(x_1, \cdots x_n)d\tau = 1} \quad \textbf{(3.14)}$$

Using the variational principle

$$\boldsymbol{\delta[\langle\psi|H|\psi\rangle - \sum_i \lambda_i \int u_i^*(x_i)u_i(x_i)d\tau] = 0} \quad \textbf{(3.15)}$$

We have

$$\boldsymbol{\epsilon_k u_k = [\frac{\nabla^2}{2} - \sum_{I=1}^{M} \frac{Z_I e^2}{|\vec{r}_k - \vec{R}_I|} + \frac{\int n(r_l)}{|r_k - r_l|} d\tau_l]u_k} \quad \textbf{(3.16)}$$

$$\boldsymbol{\epsilon_k u_k = \left[\hat{T}_e + \hat{V}_{ion} + \hat{V}_H\right]u_k} \quad \textbf{(3.17)}$$

This is called the famous independent electron approximation. The above equation can be solved self consistently.

3.4.1 Limitations of Hatree Approximation

- The trial wave function employed in the approximation has no antisymmetric property, as such does not take into account Pauli's exclusion principle.
- Moreover, with the approximation, the degree of freedom scales with the size of the system in question.

3.5 Hatree-Fock Approximation

Here, the trial many-body wavefunction is represented as a single slater determinant of N spin-orbitals.

$$\boldsymbol{\psi}(\vec{\boldsymbol{r}}_1, \vec{\boldsymbol{r}}_2, \ldots, \vec{\boldsymbol{r}}_N) = \frac{1}{\sqrt{N!}} \begin{vmatrix} \boldsymbol{\phi}_1(\vec{\boldsymbol{r}}_1) & \boldsymbol{\phi}_2(\vec{\boldsymbol{r}}_1) & \ldots. & \boldsymbol{\phi}_N(\vec{\boldsymbol{r}}_1) \\ \boldsymbol{\phi}_1(\vec{\boldsymbol{r}}_2) & \boldsymbol{\phi}_2(\vec{\boldsymbol{r}}_2) & \ldots. & \boldsymbol{\phi}_N(\vec{\boldsymbol{r}}_2) \\ . & . & \ldots. & . \\ . & . & \ldots. & . \\ . & . & \ldots. & . \\ . & . & \ldots. & . \\ \boldsymbol{\phi}_1(\vec{\boldsymbol{r}}_N) & \boldsymbol{\phi}_2(\vec{\boldsymbol{r}}_N) & \ldots. & \boldsymbol{\phi}_N(\vec{\boldsymbol{r}}_N) \end{vmatrix} \quad \textbf{(3.18)}$$

Hatree-Fock approximation accounted for the antisymmetric property of the wavefunction when the electrons change positions and it gives zero when two electrons assume the same position. Hence the Pauli's Exclusion Principle is not violated.

Applying the variational principle,

$$\boldsymbol{\delta}[\langle \boldsymbol{\psi} | \boldsymbol{H} | \boldsymbol{\psi} \rangle - \sum_i \boldsymbol{\lambda}_i \int \boldsymbol{\phi}_i^*(\boldsymbol{x}_i) \boldsymbol{\phi}_i(\boldsymbol{x}_i) \boldsymbol{d\tau}] = \mathbf{0} \quad \textbf{(3.19)}$$

we have

$$\boldsymbol{\epsilon}_i \boldsymbol{\phi}_i = \left[\widehat{\boldsymbol{T}}_e + \widehat{\boldsymbol{V}}_H + \widehat{\boldsymbol{V}}_{ion}\right] \boldsymbol{\phi}_i - \frac{1}{2} \sum_{i,j} \int \boldsymbol{d^3 r'} \boldsymbol{\phi}_j^*(\vec{\boldsymbol{r}}') \boldsymbol{\phi}_i(\vec{\boldsymbol{r}}\ ) \frac{1}{|\vec{\boldsymbol{r}} - \vec{\boldsymbol{r}}'|} \boldsymbol{\phi}_i(\vec{\boldsymbol{r}'}) \boldsymbol{\phi}_j(\vec{\boldsymbol{r}}) \quad \textbf{(3.20)}$$

Where the last term is called the exchange term

3.5.1 Limitations of Hatree-Fock Approximation

- Exchange term makes the equation difficult to solve
- The description of homogenous gases by the equation is limited
- The energy calculation from HF is always greater than ground state energy
- Lack electrons correlation

3.6 Density Functional Theory

The electron density, rather than the many-body wavefunction, is the fundamental variable in density functional theory (DFT). The density is a function of three variables, i.e., the three

Cartesian directions, rather than the maximum many-body wavefunction's 3N variables, which results in a significant reduction in complexity. Thomas and Fermi [18] suggested an early density functional theory. This took the kinetic energy to be a function of the electron density, however, like the Hartree and Hartree-Fock methods, only incorporated electron-electron interactions via a mean field potential, ignoring both exchange and correlation; a subsequent proposal by Dirac [19], formulating an expression for the kinetic energy to be a function of the electron density. The approach was not greatly improved by expressing the exchange energy in terms of the electron density. The Hohenberg-Kohn-Sham formulation of DFT is considered here. His approach is one of the most widely used state-of-the-art methods in electronic structure theory, with applications ranging from quantum chemistry to condensed matter physics to geophysics. The following remarkable and deceptively basic theorems underpin it:

- The ground state energy is a unique functional of the electron density (n®)

$$\boldsymbol{F[n] = \int dr\, n(r) V_n(r) + \langle \Psi[n] | T + V_{e-e} | \Psi[n] \rangle} \qquad \textbf{(3.21)}$$

- The ground state energy is the minimum of this functional, and the density that minimizes the functional is the ground state density

$$\textbf{E[n] =F[n]=} \int dr\, n(r) V_n(r) - \sum_i \int dr\, \phi_i^*(r) \frac{\nabla^2}{2} \phi_i(r) + \frac{1}{2} \int \int dr dr' \frac{n(r) n(r')}{|r-r'|} E_{xc}[n] \qquad \textbf{(3.22)}$$

Applying variational principle.

$$\frac{\delta F[n]}{\delta n}\Big|_{n_o} = 0 \qquad \textbf{(3.23)}$$

We have

$$\left[-\frac{1}{2}\nabla^2 + V_n(r) + V_H(r) + V_{xc}(r) \right] \phi_i(r) = \epsilon_i \phi_i \qquad \textbf{(3.24)}$$

Where,

$$V_{xc} = \frac{\delta E_{xc}[n]}{\delta n}|_{n(r)} \quad \textbf{(3.25)}$$

This is known as the Kohn-Sham Equation.

3.7 Exchange-Correlation Functional

The energy contribution from quantum effects does not included in the Coulomb repulsion and the single-particle kinetic energy is represented by the exchange-correlation term($\boldsymbol{E_{xc}[n]}$). This expression's exact form isn't known. The local density approximation (LDA), generalized gradient approximation, hybrid functional and other approximations are widely used to evaluate the exchange correlation energy.

3.7.1 The Local Density Approximation (LDA)

Local-density approximations (LDA) are a class of density functional theory (DFT) approximations to the exchange–correlation (XC) energy functional that depend exclusively on the value of the electronic density at each point in space (rather than, for example, density derivatives or Kohn–Sham orbitals).

Limitation of LDA

- Failed to predict accurately electronic properties of semiconductors such as band gaps
- Underestimation of lattice parameters
- Overestimation of cohesive energy and modulus of solids

3.7.2 The Generalized Gradient Approximation (GGA)

The exchange correlation (XC) potential in the generalized gradient approximation (GGA) to DFT is a complicated function in three-dimensional space that depends on the electron density and its gradient.

Limitations of GGA

- Slightly underestimate the band-gap of semiconductors

3.7.3 The Hybrid functionals

Hybrid functional gives accurate band gap of semi-conductors, but computationally expensive.

3.8 Plane Wave Basis Set

The electronic wavefunctions at each k-point can be generalized in terms of a discrete plane-wave base set, according to Bloch's theorem. In theory, such an expansion would require an infinite number of plane waves.

The plane wave basis set used for this work is given as:

$$\psi_j(\boldsymbol{k},\boldsymbol{r}) = \frac{1}{\sqrt{N_o\Omega}} \sum_G A_j(\boldsymbol{k}+\boldsymbol{G})\, e^{(\boldsymbol{k}+\boldsymbol{G})\cdot\boldsymbol{r}} \qquad \textbf{(3.26)}$$

3.9 Pseudopotential

Pseudopotential is used to describe the electron–ion reaction. Pseudopotentials describes the apparent weak interaction between active electrons and ion cores in solids and allows for efficient calculation of real-world properties. Pseudopotentials remove the core electrons from the model, allowing the use of considerably simpler basis sets. Types of pseudopotentials: norm conservatives, ultra-soft, projected-augmented wave (PAW)

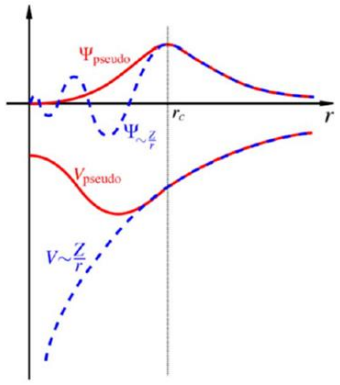

Figure 3.1 – Pseudopotentials

3.10 Self-consistent field calculation (SCF)

This process is aided using software such as VASP, Quantum Espresso, CASTEP, fhi-aims, Abinit, etc.

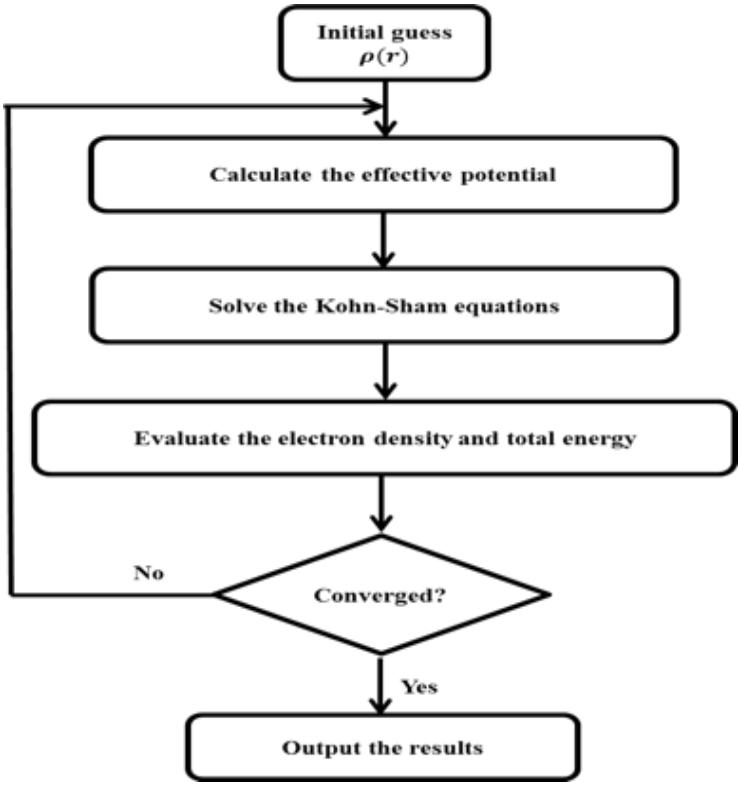

Figure 3.2 – self-consistent field calculation

3.11 Computational Details

- Density functional theory (DFT)
- Projected augmented-wave (PAW)
- VASP
- Generalized Gradient Approximation (GGA)
- Brillouin zone K-points 5x5x1 for scf; 15x15x1 for PDOS
- System size 72-atoms
- Energy cut-off 400eV with spin polarized calculation

CHAPTER FOUR

RESULTS AND DISCUSSION

4.1 Test of Convergence

The optimized structures and self-consistent calculations were computed. The test of convergence with respect to the cut-off energy and kpoints converges at 400 eV for cut-off energy and 5x5x1 for kpoints.

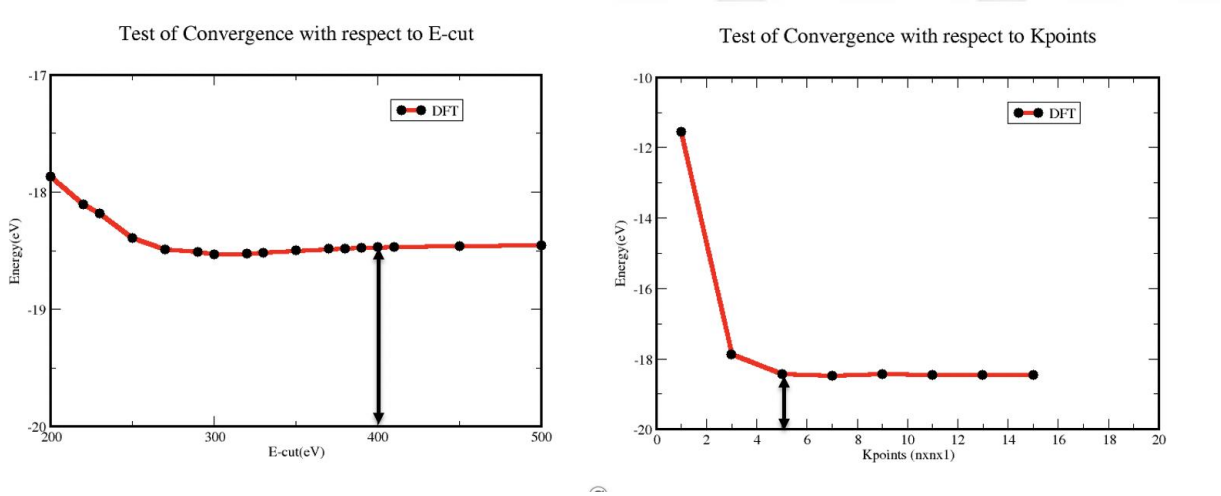

(a) **(b)**

Figure 4.1 – (a) Test of convergence with respect to the cut-off Energy (b) Test of convergence with respect to Kpoints

4.1.1 Structural Parameter of Graphene and Hexagonal Boron Nitride

In comparison with experimental data (**D. Cooper *et al.,cond. Matter physics 6(2011))*** [20] with 2.46 Å lattice constant and 1.43 Å bond length, the optimized graphene structure has lattice constant of 2.47 Å and 1.43 Å bond length. See figure 4.2

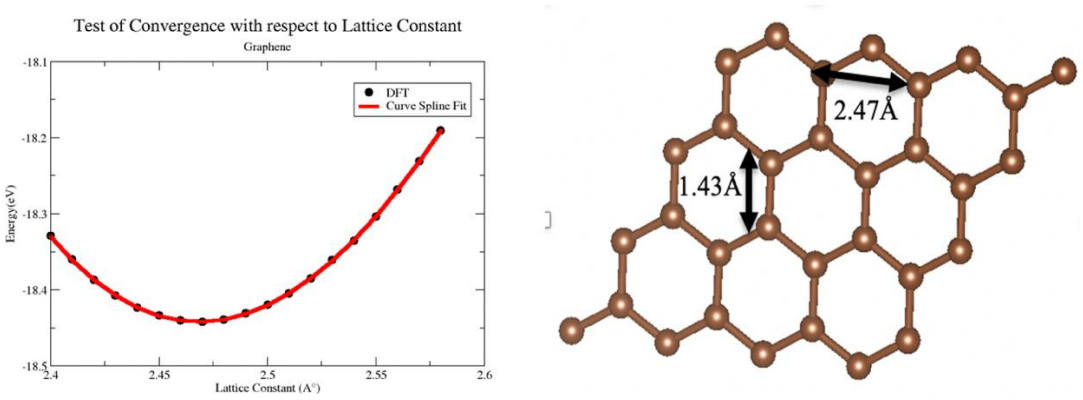

Figure 4.2 – Test of Convergence of graphene with respect to the lattice constant

Also, the experimental lattice constant of h-BN is 2.507 Å (Ooi et. al., 2006)[21]. Our optimized h-BN structure with lattice constant 2.51 Å agrees reasonably with the experimental value.

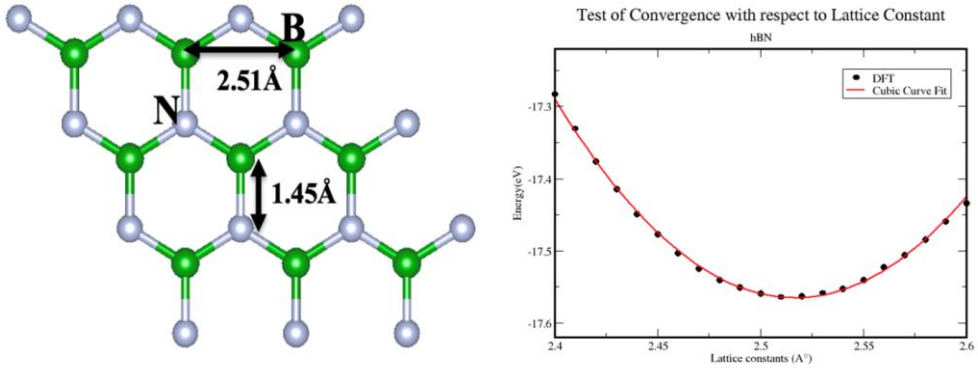

Figure 4.3 – Test of Convergence of h-BN with respect to the lattice constant

4.2 Graphene-Hexagonal Boron Nitride Hybrid

In this work, we studied hybrids system of graphene and hexagonal boron nitride.

4.2.1 Graphene Embedded in Hexagonal Boron Nitride

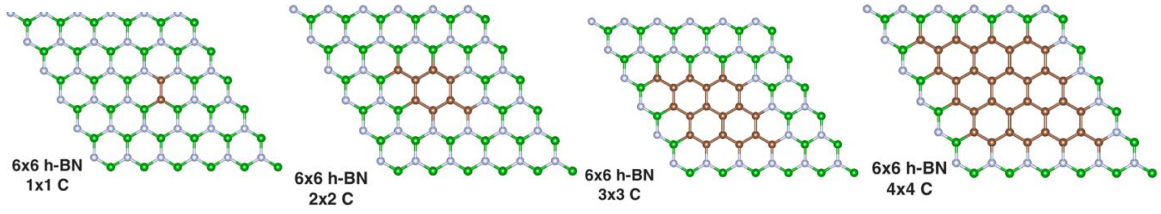

Figure 4.4 - Graphene Embedded in Hexagonal Boron Nitride Hybrids

4.2.2 Hexagonal Boron Nitride Embedded in Graphene

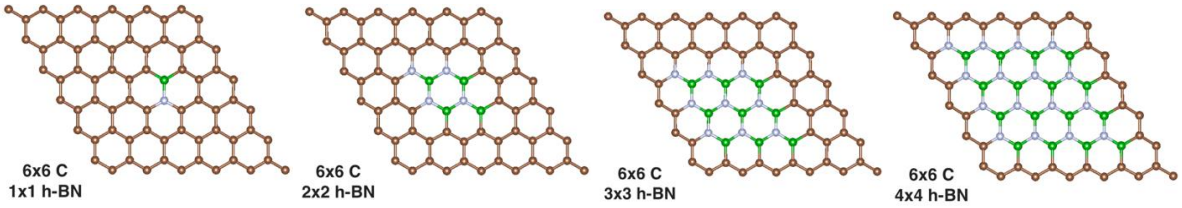

Figure 4.5 – h-BN Embedded in Graphene Hybrids

4.3 Cohesive Energy of Graphene/h-BN Hybrids

To study the stability of these hybrid systems, we calculated the cohesive energy of the systems. It is deduced that all the hybrids are stable.

For the graphene embedded in h-BN, 4x4 (7.39 eV/atom) graphene in h-BN is more stable and the 1x1 graphene in h-BN (7.07 eV/atom) is more stable than the pristine h-BN (7.06 eV/atom). Also, for h-BN in graphene, a pristine graphene(7.90 eV/atom) is more stable than the hybrids (7.85 eV/atom – 7.35 ev/atom) but the hybrids are more stable than a pristine h-BN.

- **Graphene Embedded in h-BN**

Hybrids	Cohesive Energy (eV/atom)
Pristine h-BN	7.06
1x1	7.058
2x2	7.091
3x3	7.17
4x4	7.39

Table 4.1 – Cohesive Energy of Graphene in h-BN Hybrids

- **h-BN embedded in Graphene**

Hybrids	Cohesive Energy(eV/atom)
Pristine Graphene	7.90
1x1	7.85
2x2	7.75
3x3	7.59
4x4	7.39

Table 4.2 – Cohesive Energy of h-BN in Graphene Hybrids

4.4 Electronic Structure of Graphene and h-BN

The electronic band structure and h-BN of graphene and h-BN was determined using these optimized structures. The calculations yielded a band gap of 0.0 eV and 4.5 eV respectively. This agrees with theoretical and experimentally determined band gap spectrum for h-BN (3.6-7.0 eV) and zero band gap for graphene.

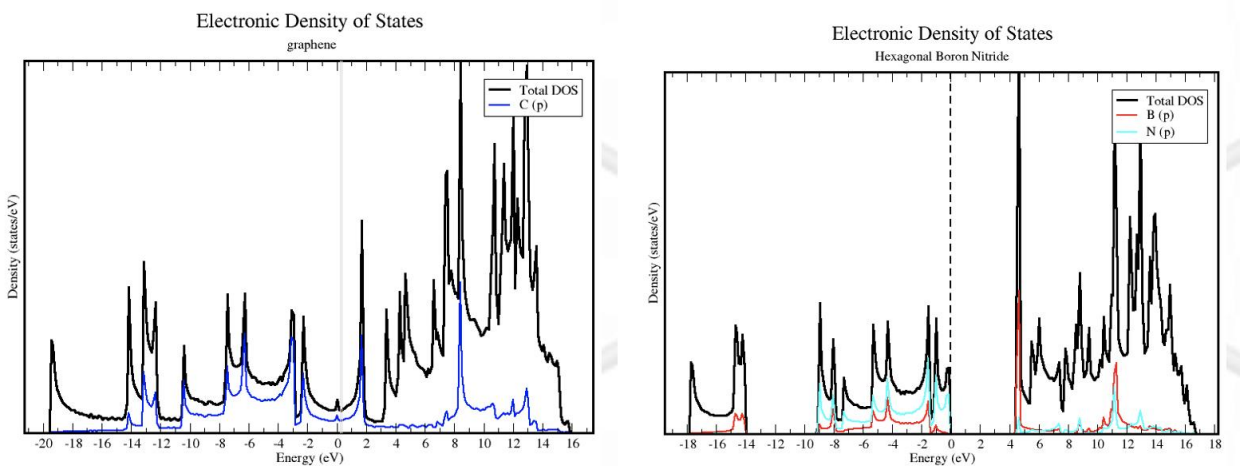

Figure 4.6 – Density of State (DOS) diagram showing the electronic structure of graphene and hexagonal boron nitride respectively.

4.5 PDOS of Graphene/h-BN Hybrid

To study the electronic structure of the hybrids system, we calculated the PDOS of these hybrids. It was discovered that increase in the concentration of h-BN in graphene increases its band gap from 0.0 eV to 1.06 eV while increase in the concentration of graphene in h-BN reduces the bang gap of graphene from 4.5 eV to 0.64 eV. This implies that the size of the band gap of the hybrid is a function of the size of graphene and h-BN in the hybrids. The band gap of graphene in h-BN hybrid decreases as more boron and nitrogen atoms are replaced with carbon atoms while the bad gap of graphene increases as more carbon atoms are replaced with boron and nitrogen atoms.

4.4.1 h-BN in Graphene

Hybrids	PDOS
1x1 h-BN in Graphene **Band gap = 0.12 eV**	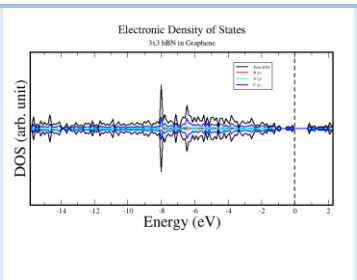
3x3 h-BN in Graphene **Band gap = 0.86 eV**	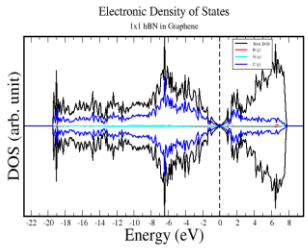
4x4 h-BN in Graphene **Band gap = 1.06 eV**	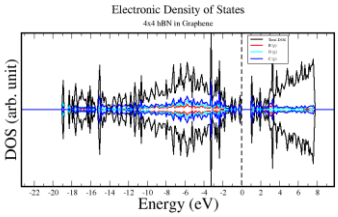

Table 4.3 – PDOS of h-BN in Graphene Hybrids

4.4.3 Graphene in h-BN

Hybrids	PDOS
1x1 Graphene in h-BN **Band gap = 3.71 eV**	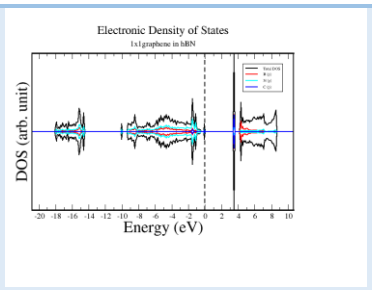
2x2 Graphene in h-BN **Band gap = 3.3 eV**	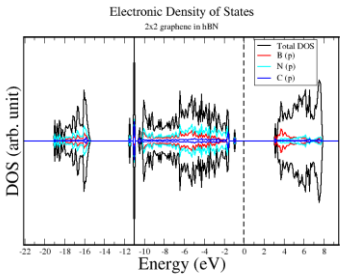
3x3 Graphene in h-BN **Band gap = 1.61eV**	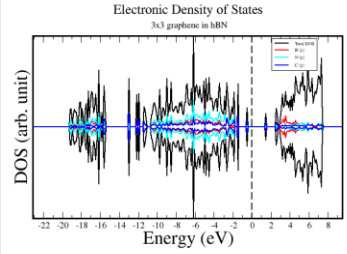
4x4 Graphene in h-BN **Band gap = 0.64 eV**	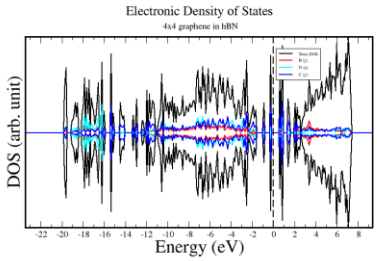

Table 4.4 –PDOS of Graphene in h-BN Hybrids

4.6 Work Function of graphene/h-BN hybrid with and without planar deformations

Work function is the measure of the minimum energy required to extract an electron from the surface of a solid.

$$W=\phi - \epsilon_f$$

Where,

ϕ **= Vacuum potential**

ϵ_f **= Fermi Energy**

4.5.1 Work Function of graphene/h-BN hybrid without planar deformations

- **Graphene Embedded in h-BN**

Hybrids	Work function (eV)
1x1	5.1893
2x2	4.3863
3x3	4.0929
4x4	4.0561

Table 4.5 – Work function of h-BN in Graphene Hybrids without planar deformations

- **h-BN embedded in Graphene**

Hybrids	Work function (eV)
Pristine Graphene	4.6
1x1	4.144
2x2	4.0979
3x3	4.1906
4x4	4.2827

Table 4.6 – Work function of h-BN in Graphene Hybrids without planar deformations

4.5.2 Work Function of graphene/h-BN hybrid with planar deformations

Uniform planar deformation

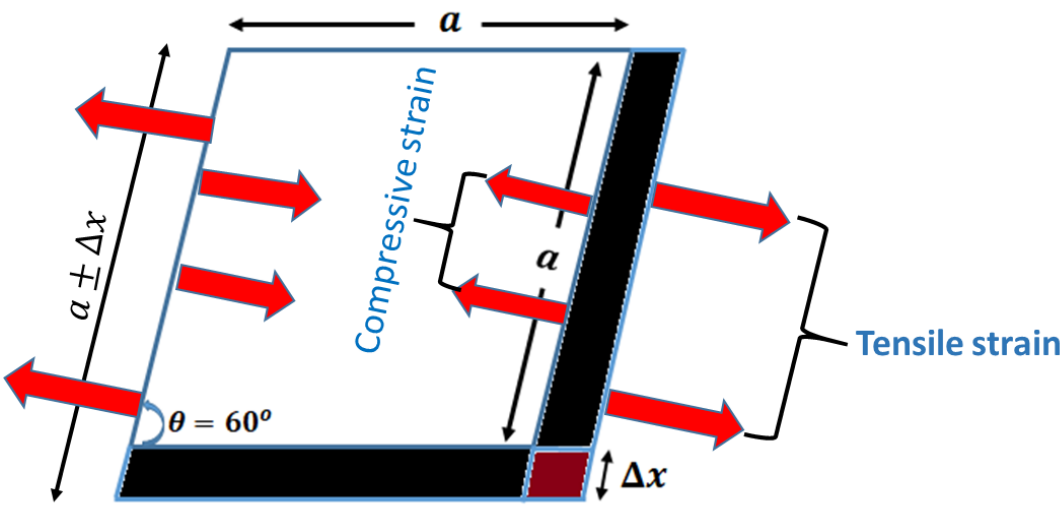

Figure 4.7 – Application of tensile strain and compressive strain on the hybrid structure

$$\epsilon = \frac{\delta A}{A} = \frac{2a\Delta x sin\theta + \Delta x^2 sin\theta}{a^2 sin\theta}$$

$$\Delta x^2 + 2a\Delta x - a^2\epsilon = 0$$

$$a + \Delta x = a\sqrt{(1+\epsilon)} \rightarrow \textbf{Tensile Strain}$$

$$a - \Delta x = a\sqrt{(1-\epsilon)} \rightarrow \textbf{Compressive Strain}$$

Considering the most stable configuration in each hybrid system

1. 1x1 h-BN embedded in Graphene
2. 4x4 Graphene embedded in h-BN

Applying up to 30 % compressive and tensile strain on these hybrids gives us a decrease in the work function for compressive strain and an increase in the work function for tensile strain.

- **1x1 h-BN embedded in 6x6 Graphene** **4x4 Graphene embedded in 6x6 h-BN**

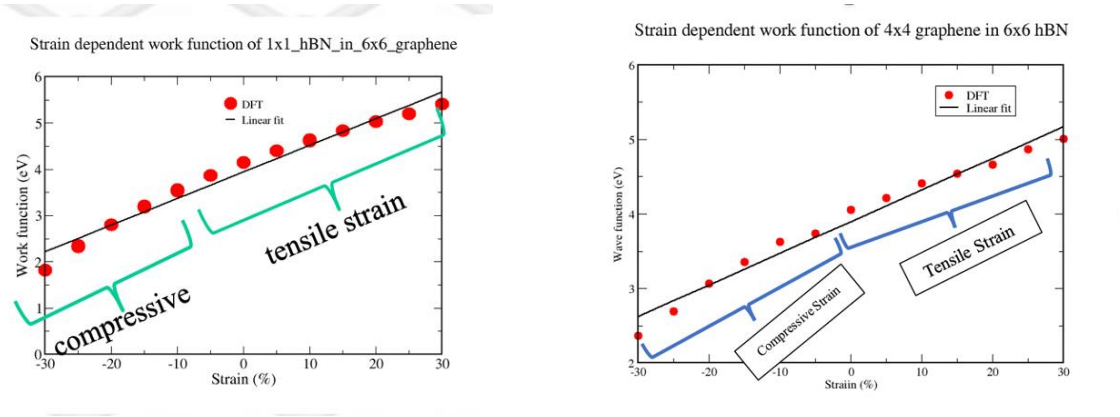

Figure 4.8 – Effect of tensile strain and compressive strain on the Work function of Graphene/h-Bn hybrids

Model Equations

WF = 0.0425ϵ + 3.8921
(1x1 h-BN in Graphene)

WF = 0.0574ϵ + 3.9463
(4x4 Graphene in h-BN)

CHAPTER FIVE

CONCLUSION AND RECOMMENDATION

CONCLUSION

- DFT was used to investigate the geometry and electronic properties of graphene/hexagonal boron nitride hybrid. The result of the study shows that the system is a semiconductor with a tunable work function. The range of work function of the material makes it applicable in a wide range of electronic applications.
    - 2.37 – 5.01 eV for 4x4 graphene in 6x6 h-BN
    - 3.86 – 5.39 eV for 1x1 h-BN in graphene
- The result of the cohesive energy reveals that the hybrid systems are very stable
- The work function-strain models derived for the hybrid systems would be useful for rational device fabrication and characterizations.
    1. **WF = 0.0425ϵ + 3.8921 → Graphene in h-BN**
    2. **WF = 0.0574ϵ + 3.9463 → h-BN in Graphene**

RECOMMENDATION

In this study, generalized gradient approximation (GGA) was used as the exchange correlation functional. Its known that GGA underestimate the band gap of semiconductors. For future study, hybrid functionals (such as HSE06) should be used because HSE06 usually gives accurate band gap of semiconductors.

References

[1] A. K. Geim and K. S. Novoselov, "The rise of graphene," *Nanosci. Technol. A Collect. Rev. from Nat. Journals*, pp. 11–19, 2009, doi: 10.1142/9789814287005_0002.

[2] A. C. Ferrari *et al.*, "Science and technology roadmap for graphene, related two-dimensional crystals, and hybrid systems," *Nanoscale*, vol. 7, no. 11, pp. 4598–4810, 2015, doi: 10.1039/c4nr01600a.

[3] M. I. Katsnelson, "The electronic structure of ideal graphene," *Graphene*, vol. 0, no. May, pp. 1–22, 2012, doi: 10.1017/cbo9781139031080.002.

[4] K. Wakabayashi, *Electronic properties of nanographene*. 2013.

[5] R. T. Paine and C. K. Narula, "Synthetic Routes to Boron Nitride," *Chem. Rev.*, vol. 90, no. 1, pp. 73–91, 1990, doi: 10.1021/cr00099a004.

[6] W. Sinclair and H. Simmons, "Microstructure and thermal shock behaviour of BN composites," *J. Mater. Sci. Lett.*, vol. 6, no. 6, pp. 627–629, 1987, doi: 10.1007/BF01770905.

[7] H. J. Xiang, E. J. Kan, S. H. Wei, X. G. Gong, and M. H. Whangbo, "Thermodynamically stable single-side hydrogenated graphene," *Phys. Rev. B - Condens. Matter Mater. Phys.*, vol. 82, no. 16, pp. 2–5, 2010, doi: 10.1103/PhysRevB.82.165425.

[8] J. Berashevich and T. Chakraborty, "Tunable band gap and magnetic ordering by adsorption of molecules on graphene," *Phys. Rev. B - Condens. Matter Mater. Phys.*, vol. 80, no. 3, pp. 1–4, 2009, doi: 10.1103/PhysRevB.80.033404.

[9] O. Olaniyan *et al.*, "Exploring the stability and electronic structure of beryllium and sulphur co-doped graphene: A first principles study," *RSC Adv.*, vol. 6, no. 91, pp. 88392–88402, 2016, doi: 10.1039/c6ra17640b.

[10] L. Ci *et al.*, “Atomic layers of hybridized boron nitride and graphene domains,” *Nat. Mater.*, vol. 9, no. 5, pp. 430–435, 2010, doi: 10.1038/nmat2711.

[11] M. H. Mohammed, “Designing and engineering electronic band gap of graphene nanosheet by P dopants,” *Solid State Commun.*, vol. 258, pp. 11–16, 2017, doi: 10.1016/j.ssc.2017.04.011.

[12] Y. Zhou *et al.*, “Tuning and understanding the supercapacitance of heteroatom-doped graphene,” *Energy Storage Mater.*, vol. 1, pp. 103–111, 2015, doi: 10.1016/j.ensm.2015.09.002.

[13] R. Beiranvand and S. Valedbagi, “Electronic and optical properties of h-BN nanosheet: A first principles calculation,” *Diam. Relat. Mater.*, vol. 58, pp. 190–195, 2015, doi: 10.1016/j.diamond.2015.07.008.

[14] B. Huang and H. Lee, “Defect and impurity properties of hexagonal boron nitride: A first-principles calculation,” *Phys. Rev. B - Condens. Matter Mater. Phys.*, vol. 86, no. 24, pp. 1–8, 2012, doi: 10.1103/PhysRevB.86.245406.

[15] M. Zhao, Y. Miao, Y. Huang, K. Xu, and F. Ma, “The effect of H adsorption on the electronic and magnetic states in the hybrid structure of graphene and BN,” *Comput. Mater. Sci.*, vol. 93, pp. 50–55, 2014, doi: 10.1016/j.commatsci.2014.06.021.

[16] O. Olaniyan, L. Moskaleva, R. Mahadi, E. Igumbor, and A. Bello, “Tuning the electronic structure and thermodynamic properties of hybrid graphene-hexagonal boron nitride monolayer,” *FlatChem*, vol. 24, no. August, 2020, doi: 10.1016/j.flatc.2020.100194.

[17] M. Legesse, S. N. Rashkeev, F. Al-Dirini, and F. H. Alharbi, “Tunable high workfunction contacts: Doped graphene,” *Appl. Surf. Sci.*, vol. 509, p. 144893, 2020, doi: 10.1016/j.apsusc.2019.144893.

[18] R. G. Parr and S. K. Ghosh, “Thomas-Fermi theory for atomic systems,” *Proc. Natl. Acad. Sci.*, vol. 83, no. 11, pp. 3577–3579, 1986, doi: 10.1073/pnas.83.11.3577.

[19] P. A. M. Dirac, “Discussion of the infinite distribution of electrons in the theory of the positron,” *Math. Proc. Cambridge Philos. Soc.*, vol. 30, no. 2, pp. 150–163, 1934, doi: 10.1017/S030500410001656X.

[20] D. R. Cooper *et al.*, “Experimental Review of Graphene,” *ISRN Condens. Matter Phys.*, vol. 2012, pp. 1–56, 2012, doi: 10.5402/2012/501686.

[21] N. Ooi, A. Rairkar, and J. B. Adams, “Density functional study of graphite bulk and surface properties,” *Carbon N. Y.*, vol. 44, no. 2, pp. 231–242, 2006, doi: 10.1016/j.carbon.2005.07.036.